

# Modelling isolated hydrogen impurity in $\text{Lu}_2\text{O}_3$ with muonium spectroscopy

Rui C. Vilão<sup>1,\*</sup>, Ricardo B. L. Vieira<sup>2</sup>, Helena V. Alberto<sup>1</sup>, João M. Gil<sup>1</sup>, Alois Weidinger<sup>3</sup>, Roger L. Lichti<sup>4</sup>, Patrick W. Mengyan<sup>4,5</sup>, Britany B. Baker<sup>6</sup>, and James S. Lord<sup>7</sup>

<sup>1</sup>CFisUC, Department of Physics, University of Coimbra, R. Larga, P-3004-516 Coimbra, Portugal

<sup>2</sup>CICECO - Aveiro Institute of Materials, Department of Chemistry, University of Aveiro, 3810-193 Aveiro, Portugal

<sup>3</sup>Helmholtz-Zentrum Berlin für Materialien und Energie, 14109 Berlin, Germany

<sup>4</sup>Department of Physics, Texas Tech University, Lubbock TX 79409-1051, USA

<sup>5</sup>Department of Physics, Northern Michigan University, Marquette, MI, 49855

<sup>6</sup>Department of Physics and Engineering, Francis Marion University, Florence, SC 29502, USA

<sup>7</sup>ISIS Facility, Rutherford Appleton Laboratory, Chilton, Didcot, Oxon OX11 0QX, United Kingdom

**Abstract.** We identified in this experiment two muon configurations in  $\text{Lu}_2\text{O}_3$ , the oxygen-bound ( $\text{O}-\text{Mu}^+$ ) ground state and a metastable (energy barrier 0.7(3) eV) atom-like excited state. These configurations are partially not formed immediately after implantation but somewhat delayed due to the requirement of a lattice rearrangement around the muon. These rearrangement processes occur on a timescale of ns to  $\mu\text{s}$  and are thus observable in  $\mu\text{SR}$  experiments. A special role plays a fairly long-lived (ns to  $\mu\text{s}$ ) transition state as an intermediate step in the reaction process.

## 1 Introduction

Oxides, including rare earth oxides, are currently under intense scrutiny in the context of applications in electronic devices [1–3]. The hydrogen impurity can have a prominent impact in the respective properties, particularly in the electrical transport [4]. Hydrogen concentrations as large as 1% can be reached, even for samples grown with high quality methods [5, 6].

The knowledge of the isolated hydrogen configurations inside the material is an essential step for the understanding of the electrical properties [7, 8]. Isolated hydrogen is however very difficult to tackle experimentally, and most information has been obtained by using muonium as a light pseudo-isotope [9]. The electronic properties of this bound state of a positive muon and an electron mimic very closely those of hydrogen, and the spectroscopy of the muon spin using implanted muons presents the further advantage of allowing to probe the ground state as well as metastable configurations (usually implied in high-temperature dynamical behaviour).

Despite their growing relevance, not much is known about the hydrogen or muonium configurations in rare-earth oxides. Thorough *ab-initio* calculations have been performed for the hydrogen impurity in the diamagnetic lutetium sesquioxide  $\text{Lu}_2\text{O}_3$  [10], which have prompted a close inspection of the corresponding experimental muonium configurations.

\*e-mail: ruivilao@uc.pt

## 2 Experimental details

A polycrystalline  $\text{Lu}_2\text{O}_3$  sample used in the present study was obtained commercially from Alfa-Aesar (REActon 99.995%). The  $\mu\text{SR}$  measurements were performed partially at TRIUMF (Vancouver, Canada) [11] and partially at ISIS (UK) [12, 13]. At TRIUMF, high-transverse field (up to 7 T) measurements were performed at the HiTime spectrometer on the M15 surface muon channel. At ISIS, low transverse field (10 mT) were obtained with the EMU spectrometer in the temperature range from 8 K to 700 K. Details of the instruments and of the  $\mu\text{SR}$  method can be found on the web pages of TRIUMF and ISIS [11, 12]. Data were analyzed with WiMDA [14].

## 3 Experimental results and discussion

Measurements in high-transverse field (Fig. 1) reveal the presence of two oscillating components of the muon spin polarization, at the muon Larmor frequency  $\nu_d = \gamma_\mu B$  (corresponding to muons with a diamagnetic surrounding), and at the frequency  $\nu_{12}$  corresponding to a muonium configuration with an isotropic hyperfine parameter  $A = 3629(2)$  MHz.

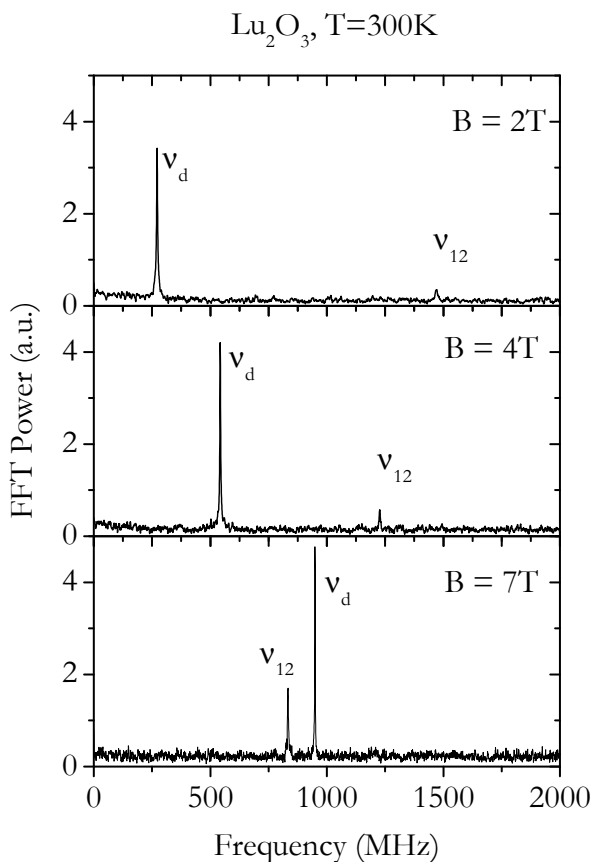


**Figure 1.** Fast-Fourier transform of high transverse-field  $\mu\text{SR}$  measurements at several applied magnetic fields. Two oscillation frequencies  $\nu_d$  and  $\nu_{12}$  are clearly seen, corresponding to a diamagnetic state and to a muonium state, respectively.

### 3.1 Oxygen-bound and atom-like muonium

We will shortly describe the two observed states:

*Oxygen-bound muonium.* The diamagnetic signal in this experiment is assigned to the configuration where the muon is bound to an oxygen atom. It corresponds to the well-known O–H donor configuration in its ionized state. This configuration was also predicted in theoretical calculations as the ground state of  $H^+$  in  $Lu_2O_3$  [10].

*Atomic muonium.* The observed state with the large and isotropic hyperfine interaction is assigned to atom-like muonium at an open interstitial site. In theoretical calculations several such sites were identified with similar formation energy and hyperfine interaction [10]. The ground-state configuration is assigned to  $H^0$  at an interstitial unoccupied oxygen site. This state is only metastable and converts to the oxygen-bound configuration at higher temperature (see below).

### 3.2 Formation probabilities

The temperature dependence of these two components was followed up to room temperature in the high-field measurements; and up to  $T = 700$  K in measurements at low transverse field (0.01 T) of the diamagnetic component only (Fig. 2). A transient component, not shown here, has also been identified. It corresponds to a weakly bound ( $\mu^+e^-$ ) configuration which acts as precursor (transition state) for the formation of the final states [15].

Muons are implanted into the target and thus react with the matrix atoms during the slowing down process. They may pick up an electron from the host and form neutral muonium or remain in the positive charge state. During the flight there is not enough time for a rearrangement of the host atoms, thus the muon in either the neutral or the positive charge state stops

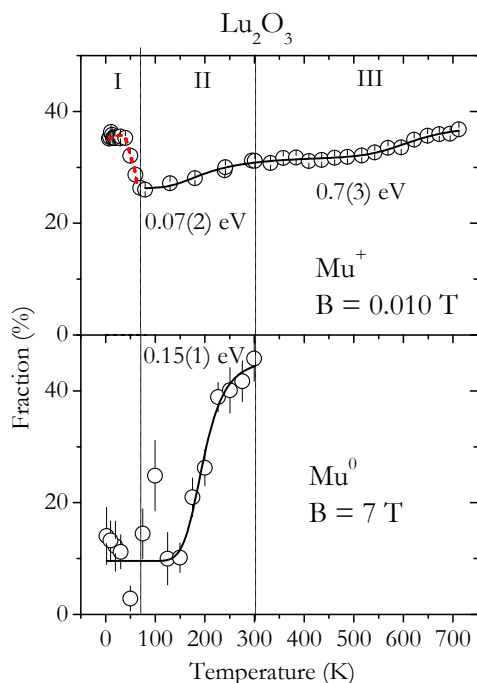


**Figure 2.** Temperature dependence of the fraction of muons stopping in the (slowly-relaxing) diamagnetic configuration  $Mu^+$  (top) and in the paramagnetic configuration  $Mu^0$  (bottom). The red dashed line is a fit to a "thermal spike model" (see below and Ref. [17]). The black lines are fits to Boltzmann functions as discussed in the text.

in the pristine lattice ( $\text{Mu}^{0*}$  or  $\text{Mu}^{+*}$ , the asterisk indicating the excited configuration). The slowing down occurs in the sub-ps time range. The subsequent reactions with the lattice are schematically indicated in Fig. 3.

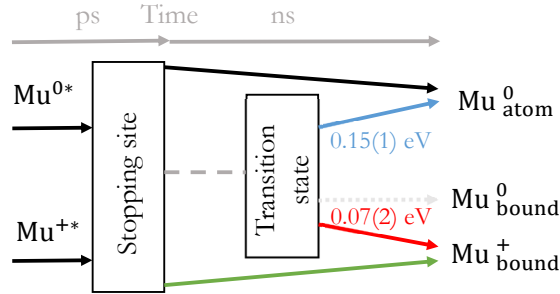


**Figure 3.** Diagram of the muon formation model based on the presence of a transition state, adapted to the  $\text{Lu}_2\text{O}_3$  case and including the possible energy barriers for the formation of the final configurations.

The stopped  $\text{Mu}^{0*}$  and  $\text{Mu}^{+*}$  may directly go to the corresponding ground states  $\text{Mu}_{\text{atom}}^0$  and  $\text{Mu}_{\text{bound}}^+$  (black and green arrow in Fig. 3). However, we recently found [16], that there is also the possibility that a fairly long-lived (ns to  $\mu\text{s}$ ) transition state is formed from which the final configurations arise (blue and red arrow). The transitions are hindered by barriers (energy values on the arrows in the Fig. 3) and are possible only at higher temperatures. This leads to the interpretation of the different temperature regions in Fig. 2.

*Region I.* The increase of the diamagnetic fraction below about 50 K is a special effect not always seen in  $\mu\text{SR}$  experiments. It is due to a local heating of the lattice by the stopping process and by stress release due to relaxation. We call it a thermal spike since it disappears quickly in particular if the temperature is increased. This excitation energy imitates a higher temperatures and can induce reactions which otherwise occur only at higher temperature [17].

*Region II.* The increase of both fractions with temperature, for the interval between 100 K and 300 K, observed in Fig. 2, has been analysed with phenomenological Boltzmann functions (Ref. [18]), which provide an estimate for the activation energies associated to the corresponding processes:  $E_a^+(\text{II}) = 0.07(2) \text{ eV}$  for the increase of the diamagnetic fraction in region II and  $E_a^0(\text{II}) = 0.15(1) \text{ eV}$  for the increase of the paramagnetic fraction in region II. We assign these reactions to the conversion of the transition state to the oxygen-bound muon (red line in Fig. 3) and the atomic muonium (blue line in Fig. 3), respectively.

*Region III.* A second step in the diamagnetic  $\text{Mu}^+$  fraction is observed in the temperature range between 300 K and 700 K (Fig. 2 top). We assign it to the ionization of ground state muonium, possibly via intermediate states, such as the oxygen-bound configuration with subsequent loss of the electron. The activation energy is  $E_a = 0.7(3) \text{ eV}$ .

## 4 Conclusions

We observe in this  $\mu\text{SR}$  experiment on  $\text{Lu}_2\text{O}_3$  two different states, one with a diamagnetic signature which we assign to the oxygen-bound ( $\text{O}-\text{Mu}^+$ ) ground state configuration, and one with an atom-like characteristic assigned to muonium at an open interstitial site. This later

state is metastable and converts at higher temperatures to the oxygen-bound configuration ( $E_a = 0.7(3)$  eV). The embedding of the muon into the host lattice requires a rearrangement of the surrounding atoms. This takes some time (ns to  $\mu$ s) and makes intermediate steps observable in  $\mu$ SR. We observed in particular i) an effect from the deposited energy at the end of the muon trajectory (thermal spike) which initiates reactions occurring otherwise only at higher temperatures, and ii) the delayed conversion from the intermediate transition state to the final configurations. Such delayed processes occur also in other implantation processes but are usually not observable. The muon as a sensitive local probe makes them visible.

## Acknowledgements

Access to the ISIS and TRIUMF beams, as well as the support of the ISIS and TRIUMF muon teams are gratefully acknowledged. This work was supported with funds from FEDER (Programa Operacional Factores de Competitividade COMPETE) and from FCT - Fundação para a Ciência e Tecnologia (Portugal) under projects UID/FIS/04564/2016 and PTDC/FIS-MAC/29696/2017.

## References

- [1] E. Fortunato, P. Barquinha, and R. Martins, *Advanced Materials* **24**, 2945 (2012).
- [2] L. Petti, N. Münzenrieder, C. Vogt, H. Faber, L. Büthe, G. Cantarella, F. Bottacchi, T. D. Anthopoulos, and G. Tröster, *Applied Physics Reviews* **3**, 021303 (2016).
- [3] R. Gillen and J. Robertson, *Microelectronic Engineering* **109**, 72 (2013).
- [4] C. G. Van de Walle and J. Neugebauer, *Annu. Rev. Mater. Res.* **36**, 179 (2006).
- [5] R. Alvero, A. Bernal, I. Carrizosa, J. A. Odriozola, and J. M. Trillo, *Journal of the Less Common Metals* **110**, 425 (1985).
- [6] J. Päiväsäari, M. Putkonen, and L. Niinistö, *Thin Solid Films* **472**, 275 (2005).
- [7] A. Weidinger, J. M. Gil, H. V. Alberto, R. C. Vilão J. Piroto Duarte, N. Ayres de Campos, and S. F. J. Cox, *Physica B: Condensed Matter* **326**, 124 (2003).
- [8] R. L. Lichti, K. H. Chow, J. M. Gil, D. L. Stripe, R. C. Vilão, and S. F. J. Cox, *Physica B: Condensed Matter* **376-377**, 587 (2006).
- [9] S. F. J. Cox, R. L. Lichti, J. S. Lord, E. A. Davis, R. C. Vilão, J. M. Gil, T. D. Veal, and Y. G. Celebi, *Physica Scripta* **88**, 068503 (2013).
- [10] E. L. da Silva, A. G. Marinopoulos, R. B. L. Vieira, R. C. Vilão, H. V. Alberto, J. M. Gil, R. L. Lichti, P. W. Mengyan, and B. B. Baker, *Phys. Rev. B* **94**, 014104 (2016).
- [11] More information at the webpage of the Centre for Molecular and Materials Science at TRIUMF: <http://musr.ca/>.
- [12] More information at the webpage of the Muon Group at the ISIS Facility: <https://www.isis.stfc.ac.uk/Pages/Muons.aspx>.
- [13] R. C. Vilão, J. S. Lord, J. M. Gil, H. V. Alberto, and J. Piroto Duarte, *STFC ISIS Neutron and Muon Source* (2012), <https://doi.org/10.5286/ISIS.E.24089275>.
- [14] F. L. Pratt, *Physica B (Amsterdam)* **289-290**, 710 (2000).
- [15] R. C. Vilão, R. B. L. Vieira, H. V. Alberto, J. M. Gil, A. Weidinger, R. L. Lichti, P. W. Mengyan, B. B. Baker, and J. S. Lord, *Phys. Rev. B* **98**, 115201 (2018).
- [16] R. C. Vilão, R. B. L. Vieira, H. V. Alberto, J. M. Gil, and A. Weidinger, *Phys. Rev. B* **96**, 195205 (2017).
- [17] R. C. Vilão, H. V. Alberto, J. M. Gil, and A. Weidinger, *Phys. Rev. B* **99**, 195206 (2019).
- [18] R. C. Vilão, A. G. Marinopoulos, R. B. L. Vieira, A. Weidinger, H. V. Alberto, J. P. Duarte, J. M. Gil, J. S. Lord, and S. F. J. Cox, *Phys. Rev. B* **84**, 045201 (2011).